



The functions of key residues in the inhibitor, substrate and cofactor sites of human 3 β -hydroxysteroid dehydrogenase type 1 are validated by mutagenesis

James L. Thomas^{a,b,*}, Vance L. Mack^a, Jingping Sun^a, J. Ross Terrell^c, Kevin M. Bucholtz^c

^a Division of Basic Medical Sciences, Mercer University School of Medicine, 1550 College St, Macon, GA 31207, United States

^b Department of Ob-Gyn, Mercer University School of Medicine, 1550 College St, Macon, GA 31207, United States

^c Department of Chemistry, Mercer University, 1400 Coleman Av, Macon, GA 31207, United States

ARTICLE INFO

Article history:

Received 14 January 2010

Received in revised form 15 April 2010

Accepted 17 April 2010

Keywords:

3 β -Hydroxysteroid dehydrogenase
Short-chain dehydrogenase/reductase
Mutagenesis
Structure–function relationship

ABSTRACT

In postmenopausal women, human 3 β -hydroxysteroid dehydrogenase type 1 (3 β -HSD1) is a critical enzyme in the conversion of DHEA to estradiol in breast tumors, while 3 β -HSD2 participates in the production of cortisol and aldosterone in the human adrenal gland. The goals of this project are to determine if Arg195 in 3 β -HSD1 vs. Pro195 in 3 β -HSD2 in the substrate/inhibitor binding site is a critical structural difference responsible for the higher affinity of 3 β -HSD1 for inhibitor and substrate steroids compared to 3 β -HSD2 and whether Asp61, Glu192 and Thr8 are fingerprint residues for cofactor and substrate binding using site-directed mutagenesis. The R195P-1 mutant of 3 β -HSD1 and the P195R-2 mutant of 3 β -HSD2 have been created, expressed, purified and characterized kinetically. Dixon analyses of the inhibition of the R195P-1 mutant, P195R-2 mutant, wild-type 3 β -HSD1 and wild-type 3 β -HSD2 by trilostane has produced kinetic profiles that show inhibition of 3 β -HSD1 by trilostane (K_i = 0.10 μ M, competitive) with a 16-fold lower K_i and different mode than measured for 3 β -HSD2 (K_i = 1.60 μ M, noncompetitive). The R195P-1 mutation shifts the high-affinity, competitive inhibition profile of 3 β -HSD1 to a low-affinity (trilostane K_i = 2.56 μ M), noncompetitive inhibition profile similar to that of 3 β -HSD2 containing Pro195. The P195R-2 mutation shifts the low-affinity, noncompetitive inhibition profile of 3 β -HSD2 to a high-affinity (trilostane K_i = 0.19 μ M), competitive inhibition profile similar to that of 3 β -HSD1 containing Arg195. Michaelis–Menten kinetics for DHEA, 16 β -hydroxy-DHEA and 16 α -hydroxy-DHEA substrate utilization by the R195P-1 and P195R-2 enzymes provide further validation for higher affinity binding due to Arg195 in 3 β -HSD1. Comparisons of the Michaelis–Menten values of cofactor and substrate for the targeted mutants of 3 β -HSD1 (D61N, D61V, E192A, T8A) clarify the functions of these residues as well.

© 2010 Elsevier Ltd. All rights reserved.

1. Introduction

Human 3 β -hydroxysteroid dehydrogenase/Delta 5 \rightarrow 4-isomerase type 1 (3 β -HSD1; short-chain dehydrogenase/reductase (SDR) nomenclature: 3BHS1_HUMAN or SDR11E1) and 3 β -hydroxysteroid dehydrogenase/Delta 5 \rightarrow 4-isomerase type 2 (3 β -HSD2; SDR nomenclature: 3BHS2_HUMAN or SDR11E2) are encoded by two distinct genes which are expressed in a tissue-specific pattern [1,2]. Both isoforms of the enzyme catalyze the conversion of 3 β -hydroxy-5-ene-steroids (dehydroepiandrosterone, 17 α -hydroxypregnenolone, pregnenolone) to 3-oxo-4-ene-steroids (androstenedione, 17 α -hydroxyprogesterone, progesterone) on a single, dimeric protein

containing both enzyme activities [3]. In addition to placenta and other human peripheral tissues, 3 β -HSD1 is selectively expressed in mammary glands and breast tumors [4], where it catalyzes the first step in the conversion of dehydroepiandrosterone (DHEA) to estradiol to promote tumor growth. In human adrenals, 3 β -HSD2 is required for the production of cortisol and aldosterone [5]. The selective inhibition of human 3 β -HSD1 in breast tumors represents a potential new treatment for hormone-sensitive breast cancer. Our studies of the structure/function of human 3 β -HSD took a dramatic turn in 2002 when we discovered a 4–16-fold higher affinity of purified human 3 β -HSD1 for substrate (DHEA) and inhibitor steroids, respectively, compared to human 3 β -HSD2 [6]. Identifying fingerprint residues that interact with key groups on inhibitors, substrates and cofactors may determine the structural basis of the higher affinity of 3 β -HSD1 for ligands relative to 3 β -HSD2. Human 3 β -hydroxysteroid dehydrogenase is a member of the short-chain dehydrogenase/reductase (SDR) family of enzymes – all of which contain the Rossmann-fold domain with a β - α - β - α - β - α - β - α - β folding pattern that binds cofactor and substrate

* Corresponding author at: Division of Basic Medical Sciences, Mercer University School of Medicine, 1550 College St, Macon, GA 31207, United States.
Tel.: +1 478 301 4177; fax: +1 478 301 5489.

E-mail address: Thomas.J@mercer.edu (J.L. Thomas).

[7]. The Rossmann-fold (residues 1–200 in 3 β -HSD) contains the YXXSK catalytic domain and shares many common fingerprint residues [8–10] that contact bound cofactor and substrate. This highly conserved domain makes human 3 β -HSD, a microsomal and mitochondrial protein which has resisted crystallization over 10 years of concerted effort, very amenable to structural homology modeling.

We have reported that our structural model is consistent with mutagenesis results showing that Tyr154 and Lys158 are the catalytic residues of human 3 β -HSD [6], Asn100 participates in catalysis [9], Cys83 is a key cofactor-binding residue [11] and Ser124 interacts with the 3 β -hydroxyl group of the DHEA substrate and the 2 α -cyanogroup of trilostane [8,12]. These amino acids are within the Rossmann-fold domain and perform similar functions in many other members of the SDR family of enzymes [10]. The aims of this project are to determine whether Arg195 in 3 β -HSD1 vs. Pro195 in 3 β -HSD2 in the substrate/inhibitor binding site is a critical structural difference responsible for the higher affinity of 3 β -HSD1 for inhibitor and substrate steroids compared to 3 β -HSD2. In addition, our structural model suggests that Asp61 and Glu192 may be fingerprint residues for cofactor or substrate binding and that Thr8 is not a critical residue in 3 β -HSD, unlike in some SDR proteins [10]. To test these ideas, the R195P-1 mutant of 3 β -HSD1, the P195R-2 mutant of 3 β -HSD2 and the targeted mutants of 3 β -HSD1 (D61N, D61V, E192A and T8A) have been created, expressed, purified and characterized kinetically.

2. Methods and materials

2.1. Chemicals

Dehydroepiandrosterone (DHEA), testosterone and pyridine nucleotides were purchased from Sigma Chemical Co. (St. Louis, MO); 5-androstene-3,17-dione from Steraloids Inc. (Newport, RI); reagent grade salts, chemicals and analytical grade solvents from Fisher Scientific Co. (Pittsburgh, PA). Glass distilled, deionized water was used for all aqueous solutions.

2.2. Bioinformatics/computational biochemistry/graphics

As described previously [9], a three-dimensional model of human 3 β -HSD1 has been developed based upon the X-ray structures of two related SDR enzymes: the ternary complex of *E. coli* UDP-galactose 4-epimerase (UDPGE) with NAD⁺ cofactor and substrate (PDB AC: 1NAH) [13] and the ternary complex of human 17 β -hydroxysteroid dehydrogenase type 1 (17 β -HSD1) with NADP and androstenedione (PDB AC: 1QYX) [14]. In this spliced model, the 153 residue N-terminal sequence comprising the NAD⁺ binding site of 3 β -HSD better matches that of UDPGE (52% homology). The substrate portion of the 3 β -HSD active site (residues 154–255) better matches that of 17 β -HSD1 (55% homology), which shares a steroid ligand specificity and dehydrogenase function with 3 β -HSD1 [9]. Amino acid sequence alignments were performed using CLUSTAL W (1.81) multiple sequence alignment [15].

This PDB file for 3 β -HSD1 was used in Autodock 3.0 (The Scripps Research Institute, <http://autodock.scripps.edu>) [16] after the 17 β -HSD product steroid was removed, leaving the NAD⁺ cofactor in the binding site. All docking experiments were carried out on Autodock 3.0 using the Genetic Algorithm with Local Searching. Independent runs (256) were carried out and the docking results were then analyzed by a ranked cluster analysis. Compounds were identified that had the lowest overall binding energy. The three-dimensional graphics of 3 β -HSD1 or the R195P-1 mutant docked with trilostane, DHEA or 16 β -hydroxy-DHEA were created using the DeepView Swiss-PdbViewer (<http://www.exspasy.org/spdbv/>) for the protein

Table 1
Oligonucleotide primers used for site-directed mutagenesis.

Mutation	Direction	Nucleotide sequence of primer ^a
R195P	Forward	5'-AGGAAGCCATTCTCTGCTAG-3'
	Reverse	5'-AAAGGAATGGGCTTCTCCCATAG-3'
P195R	Forward	5'-AGGAGGCCGATTCTCTTCTGCCAG-3'
	Reverse	5'-AAGGAATCGGCTTCTCCCATAG-3'
D61V	Forward	5'-CTGGAAGGAGTCATTCTGGATGAG-3'
	Reverse	5'-ATCCAGAATGACTCCTTCCAGCAC-3'
D61N	Forward	5'-GCTGGAAGGAAACATTCTGGATGAGC-3'
	Reverse	5'-TCCAGAATGTTTCTTCCAGCACTGTC-3'
T8A	Forward	5'-CTTGTGGCAGGAGCAGGAGGGTTTC-3'
	Reverse	5'-TGCTCTGCCACAAGGCAGCTC-3'
E192A	Forward	5'-TATGGGGCAGGAAGCCGATTCTTTCTG-3'
	Reverse	5'-GCTTCTGCCCATAGATATACATGGGTC-3'

^a The mutated codons are underlined.

with ligands and using Adobe Photoshop Elements (San Jose, CA) for text labeling.

2.3. Site-directed mutagenesis

Using the Advantage cDNA PCR kit (BD Biosciences Clontech, Palo Alto, CA) and pGEM-3 β HSD1 or pGEM-3 β HSD2 as template [17], double-stranded PCR-based mutagenesis was performed with the primers listed in Table 1 to create the cDNA encoding the R195P mutant of 3 β -HSD1, P195R mutant of 3 β -HSD2, and the D61N, D61V, T8A, E192A mutants of 3 β -HSD1. The presence of the mutated codon and integrity of the entire mutant 3 β -HSD cDNA were verified by automated dideoxynucleotide DNA sequencing using the Big Dye Terminator Cycle Sequencing Ready Reaction kit (PE Applied Biosystems, Foster City, CA). Chou-Fasman and Garnier-Osguthorpe-Robson analysis of each mutant enzyme was used to choose amino acid substitutions that produced no apparent changes in the secondary structure of the protein (Prolyze program, Scientific and Educational Software, State Line, PA).

2.4. Expression and purification of the mutant and wild-type enzymes

The mutant 3 β -HSD1 cDNA was introduced into baculovirus as previously described [17]. Recombinant baculovirus was added to 1.5×10^9 Sf9 cells (1 L) at a multiplicity of infection of 10 for expression of each mutant enzyme. The expressed mutant and wild-type enzymes were separated by SDS-polyacrylamide (12%) gel electrophoresis, probed with anti-3 β -HSD polyclonal antibody and detected using the ECL western blotting system with antigoat, peroxidase-linked secondary antibody (both from Novus Biologicals, Littleton, CO). Each expressed enzyme was purified from the 100,000 \times g pellet of the Sf9 cells (4L) by our published method [3] using Igepal CO 720 (Rhodia, Inc., Cranbury, NJ) instead of the discontinued Emulgen 913 detergent (Kao Corp, Tokyo). Each expressed, purified mutant and wild-type enzyme produced a single major protein band (42.0 kDa) on SDS-polyacrylamide (12%) gel electrophoresis that co-migrated with the purified human 3 β -HSD1 control enzyme. Protein concentrations were determined by the Bradford method using bovine serum albumin as the standard [18].

2.5. Kinetic studies

Michaelis–Menten kinetic constants for the 3 β -HSD substrate were determined for the purified mutant and wild-type enzymes in incubations containing dehydroepiandrosterone

(DHEA, 2–100 μM) plus NAD^+ (0.2 mM) and purified enzyme (0.03 mg) at 27 °C in 0.02 M potassium phosphate, pH 7.4. The slope of the initial linear increase in absorbance at 340 nm per min (due to NADH production) was used to determine 3 β -HSD1 activity. Kinetic constants for the isomerase substrate were determined at 27 °C in incubations of 5-androstene-3,17-dione (20–100 μM), with or without NADH (0.05 mM) and purified enzyme (0.02 mg) in 0.02 M potassium phosphate buffer, pH 7.4. Isomerase activity was measured by the initial absorbance increase at 241 nm (due to androstenedione formation) as a function of time. Blank assays (zero-enzyme, zero-substrate) assured that specific isomerase activity was measured as opposed to non-enzymatic, “spontaneous” isomerization [19]. Changes in absorbance were measured with a Varian (Sugar Land, TX) Cary 300 recording spectrophotometer. The Michaelis–Menten constants (K_m , V_{max}) were calculated from Lineweaver–Burke (1/S vs. 1/V) plots and verified by Hanes–Wolf (S vs. S/V) plots. The k_{cat} values (min^{-1}) were calculated from the V_{max} values (nmol/min/mg) and represent the maximal turnover rate (nmol product formed/min/nmol enzyme dimer).

Kinetic constants for the 3 β -HSD cofactor were determined for the purified mutant and wild-type enzymes in incubations containing NAD^+ (10–200 μM), DHEA (100 μM) and purified enzyme (0.03 mg) in 0.02 M potassium phosphate, pH 7.4, at 27 °C using the spectrophotometric assay at 340 nm. Kinetic constants for the isomerase cofactor as an allosteric activator were determined in incubations of NADH (0–50 μM), 5-androstene-3,17-dione (100 μM) and purified enzyme (0.02 mg) in 0.02 M potassium phosphate buffer, pH 7.4 at 27 °C using the spectrophotometric assay at 241 nm. Zero-coenzyme blanks were used as described above for the substrate kinetics.

Inhibition constants (K_i) were determined for the inhibition of the 3 β -HSD1, 3 β -HSD2, R195P-1 and P195R-2 activities by trilostane using conditions that were appropriate for each enzyme species based on substrate K_m values. For 3 β -HSD1 and P195R-2, the incubations at 27 °C contained sub-saturating concentrations of DHEA (4.0 or 8.0 μM), NAD^+ (0.2 mM), purified human type 1 enzyme (0.03–0.04 mg) and trilostane (0–1.0 μM) in 0.02 M potassium phosphate buffer, pH 7.4. For 3 β -HSD2 and R195P-1, similar incubations contained DHEA (8.0 or 20.0 μM) and trilostane (0–7.5 μM). Dixon analysis (I vs. 1/V) was used to determine the type or mode of inhibition (competitive, noncompetitive) and calculate the inhibition constant (K_i) values [20,21]. The Dixon plot is widely used to characterize enzyme inhibition kinetics and is preferable to direct binding analysis, which only determines a

dissociation constant for the inhibitor as a ligand and does not determine the type of inhibition. The K_i value represents the inhibitor concentration that reduces maximal enzyme activity by 50% and is considered a measure of the affinity of the enzyme for the inhibitor. A decrease in K_i indicates an increase in affinity [20]. Our triplicate (K_i) or duplicate (K_m) determinations of the kinetic constants used highly purified mutant and wild-type enzymes to produce very reliable results with little variation between the replicate values.

3. Results

3.1. Targeting the Arg195, Asp61, Glu192 and Thr8 residues using the structural model and docking analysis

The targeting of Arg195/Pro195 in 3 β -HSD1/3 β -HSD2 and of Thr8, Asp61 and Glu192 in 3 β -HSD1 are based on the docking results obtained with our structural model of human 3 β -HSD1, which has 51% homology of the Rossmann-fold domain (residues 1–200) and 40% identity of the key fingerprint residues that interact with bound substrate and cofactor compared to the crystallographic structure of *E. coli* UDP-galactose-4-epimerase with the substrate domain of human 17 β -hydroxysteroid dehydrogenase type 1 (17 β -HSD1) [9]. Site-directed mutagenesis has supported the function of the catalytic residues and selected substrate, cofactor and inhibitor binding residues as suggested by the structural model in previous studies [6,8,9,11,12,21]. However, we recognize the limitations of using our structural model of human 3 β -HSD1 in the docking studies. The bond distances noted below between the docked ligands (trilostane, DHEA and 16 β -hydroxy-DHEA) and the protein amino acids or NAD^+ (in the crystal structures of the enzymes used in the model) should be considered to be estimates in the absence of an actual crystallographic structure of 3 β -HSD1 with each bound steroid ligand. The structural model only suggests which amino acids to target, and the functions of these residues are then tested by mutagenesis and kinetic analyses.

In the current study, trilostane was docked in the active site of our structural model of human 3 β -HSD1 and the chimeric R195P-1 mutant of 3 β -HSD1 (containing Pro195 as in 3 β -HSD2) using Autodock 3.0. As shown in Fig. 1A, the 17 β -hydroxyl group of trilostane is proposed to interact with the R-guanidinium group of Arg195 (4.0 Å) in wild-type 3 β -HSD1. Docking with the R195P-1 mutant suggests that Pro195 in 3 β -HSD2 does not function as a recognition residue for the 17 β -hydroxyl group of trilostane (Fig. 1B).

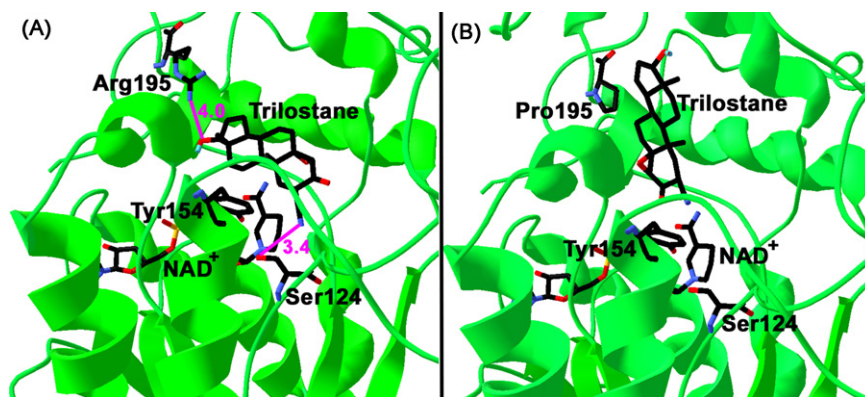


Fig. 1. Docking of trilostane with our structural model of human 3 β -HSD1. (A) The proposed interaction between the 17 β -hydroxyl group of trilostane and the guanidinium group of the Arg195 residue of the wild-type enzyme (4.0 Å) and the apparent proximity of the anchoring hydroxyl group of the Ser124 residue to the 2 α -cyanogroup of docked trilostane (3.4 Å) are shown. (B) Docking of trilostane with the R195P mutant of 3 β -HSD1 (containing Pro195) shows a binding shift of the inhibitor compared to the orientation of trilostane docked with wild-type 3 β -HSD1 containing Arg195 in Panel A. The illustrations of catalytic residues, Tyr154 and Ser124, and cofactor, NAD^+ , indicate that this view represents the active site of the enzyme. The protein backbone (green), carbon (black), oxygen (red) and nitrogen (blue) atoms plus estimated bond distances (magenta) are shown. (For interpretation of the references to color in this figure legend, the reader is referred to the web version of the article.)

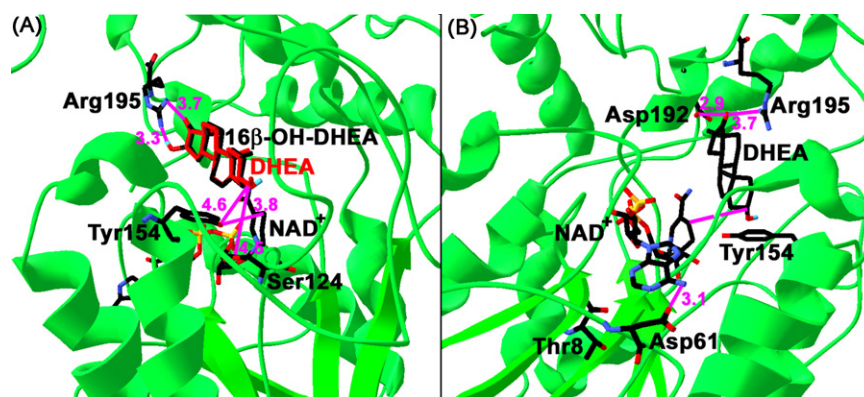


Fig. 2. Docking of 16 β -hydroxy-DHEA and DHEA with our structural model of human 3 β -HSD1. (A) The proposed dual interaction of the guanidinium group of Arg195 with the 17-keto (3.7 Å) and 16 β -hydroxyl (3.3 Å) groups of 16 β -hydroxy-DHEA is shown. The apparent proximities of the 3 β -hydroxyl group of the docked DHEA substrate to the catalytic hydroxyl group of Tyr154 (4.6 Å) and the hydroxyl group of Ser124 (4.5 Å) are shown. The apparent orientation of the catalytic nicotinamide carbon 4 of NAD⁺ (3.8 Å) to the catalytic hydroxyl group of Tyr154 is illustrated. (B) The R-carboxylate group of Glu192 is apparently positioned to interact with 17-keto-group of bound DHEA substrate (2.9 Å) as well as the R-guanidinium group of Arg195 (3.7 Å). The 6-amino group on the adenine of NAD⁺ is apparently oriented near the R-carboxylate group of Asp61 in human 3 β -HSD1 (3.1 Å). The apparent bond distance between the nicotinamide C4 of NAD⁺ and the C3 of DHEA (4.2 Å) illustrates the orientation of the enzyme active site. The Thr8 residue in wild-type 3 β -HSD1 is also shown. The protein backbone (green), carbon (black), oxygen (red) and nitrogen (blue) atoms plus estimated bond distances (magenta) are shown. (For interpretation of the references to color in this figure legend, the reader is referred to the web version of the article.)

Docking of 16 β -hydroxy-DHEA with 3 β -HSD1 estimates a dual interaction of Arg195 with the 17-keto (3.7 Å) and 16 β -hydroxyl (3.3 Å) groups of this substrate analog that may increase the affinity of the enzyme for substrate compared to DHEA with the 17-keto group alone (Fig. 2A). The 16 α -hydroxy-DHEA substrate docks very similarly to DHEA and 16 β -hydroxy-DHEA except that the 16 α -hydroxy-group is apparently oriented farther away from the R-guanidinium group of Arg195 (4.7 Å, not shown). To test our proposal that Arg195 functions as a key recognition residue for the high-affinity inhibition of 3 β -HSD1 by trilostane and for substrate utilization, the R195P-1 mutant of 3 β -HSD1 and the P195R-2 mutant of 3 β -HSD2 have been created, expressed, purified and characterized. As shown in Fig. 2B, the R-carboxylate group of Glu192 may interact with 17-keto-group of bound DHEA substrate (2.9 Å) as well as the R-guanidinium group of Arg195 (3.7 Å) accord-

ing to our docking analysis. The 6-amino group on the adenine of NAD⁺ may interact with the R-carboxylate group of Asp61 in human 3 β -HSD1 (3.1 Å). The R-hydroxyl group of Thr8 in wild-type 3 β -HSD1 is unlikely to interact with that 6-amino group (9.5 Å, not shown) of NAD⁺ (Fig. 2B). The kinetic analyses described below for the chimeric R195P-1 and P195R-2 mutant enzymes as well as of the D61V, D61N, T8A and E192A mutants of 3 β -HSD1 evaluate the functions of these amino acids.

3.2. Site-directed mutagenesis, expression and purification of the mutant enzymes

As shown by the immunoblots in Fig. 3A, the baculovirus system successfully expressed a single R195P-1 or P195R-2 mutant enzyme protein as well as wild-type human 3 β -HSD1, 3 β -HSD2 in

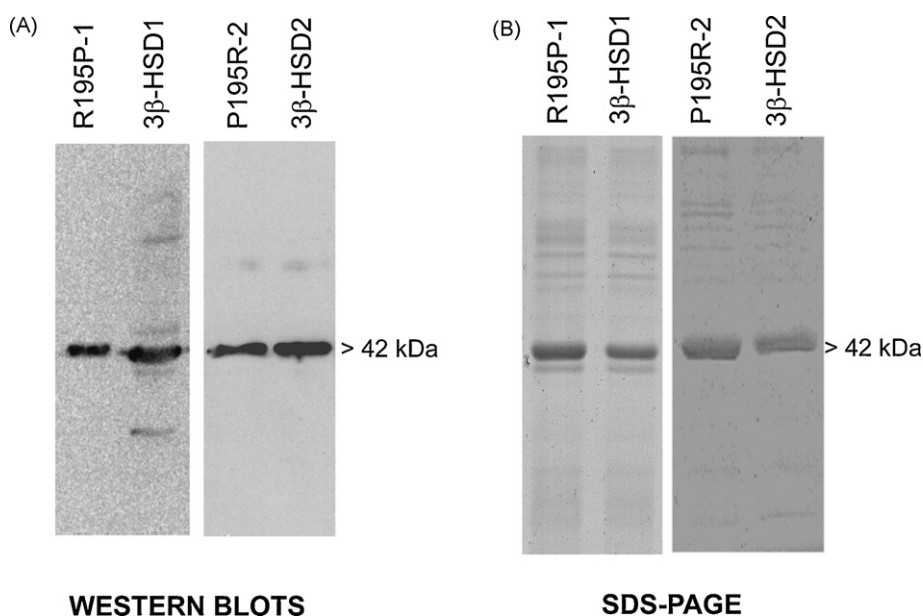


Fig. 3. Western immunoblots and SDS-Polyacrylamide gel electrophoresis of the expressed R195P-1, P195R-2 mutant and wild-type 3 β -HSD1 and 3 β -HSD2 enzymes. (A) The Sf9 cell homogenate (4.0 μ g) containing the R195P-1 or P195R-2 mutant or the purified control wild-type 3 β -HSD1 or 3 β -HSD2 enzyme (0.05 μ g) was separated by SDS-polyacrylamide (7.5%) gel electrophoresis in these western immunoblots. The 42.0 kDa band of the enzyme monomer was detected using anti-3 β -HSD antibody as described in the text. (B) SDS-polyacrylamide (7.5%) gel electrophoresis of the purified R195P-1, P195R-2 mutant and wild-type enzymes. Each lane was overloaded with 4.0 μ g of purified protein, and the bands were visualized by Coomassie Blue staining.

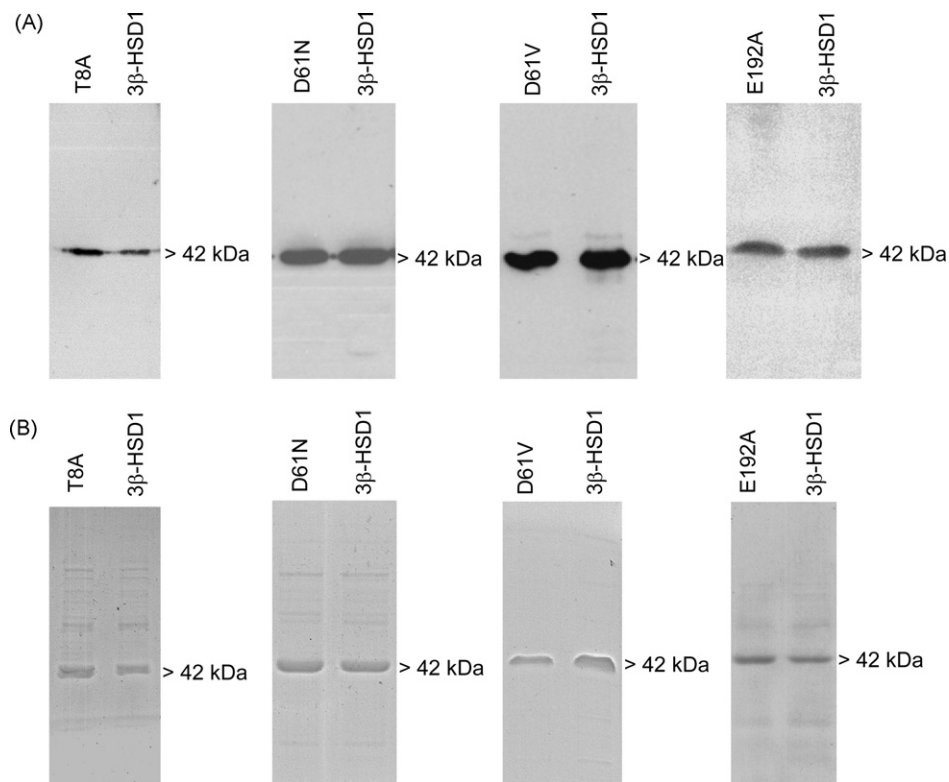


Fig. 4. Western immunoblots and SDS-Polyacrylamide gel electrophoresis of the expressed T8A, D61N, D61V, E192A mutant and wild-type 3 β -HSD1 enzymes. (A) The Sf9 cell homogenate (4.0 μ g) containing each mutant enzyme or the purified control wild-type 3 β -HSD1 (0.05 μ g) was separated by SDS-polyacrylamide (7.5%) gel electrophoresis in these western immunoblots. The 42.0 kDa band of the enzyme monomer was detected using anti-3 β -HSD antibody as described in the text. (B) The purified mutant or control wild-type enzyme was separated by SDS-Polyacrylamide (7.5%) gel electrophoresis. Each lane was overloaded with 4.0 μ g of purified protein, and the bands were visualized by Coomassie Blue staining.

Sf9 cells. Each expressed 3 β -HSD enzyme (42 kDa monomer) was highly purified (90–95%) according to protein bands visible in SDS-PAGE (Fig. 3B) using our published method [3]. These same methods were used to express the D61V, D61N, T8A and E192A mutants of 3 β -HSD1 (western immunoblots in Fig. 4A) and purify the mutant proteins (SDS-PAGE gels in Fig. 4B).

3.3. Kinetic analyses of the R195P-1 and P195R-2 mutant enzymes

Dixon analyses of the inhibition of the R195P-1 mutant, P195R-2 mutant, wild-type 3 β -HSD1 and wild-type 3 β -HSD2 by trilostane have measured inhibition constants (K_i values in Table 2) that support a role for Arg195 in the competitive inhibition of 3 β -HSD1 by trilostane with a 16-fold lower K_i compared to the noncompetitive inhibition of 3 β -HSD2 with Pro195 at this position in the

Table 2

Comparison of inhibition constants of trilostane for purified human R195P-1, 3 β -HSD1, P195R-2 and 3 β -HSD2.

Enzyme	Trilostane K_i (μ M) ^a
R195P-1	2.56 (0.22)
3 β -HSD1	0.10 (0.01) (C)
P195R-2	0.19 (0.02) (C)
3 β -HSD2	1.60 (0.10)

^a For 3 β -HSD1 and P195R-2, the incubations contained sub-saturating concentrations of DHEA (4.0 or 8.0 μ M), NAD⁺ (0.2 mM), purified human 3 β -HSD type 1 enzyme (0.04 mg) and trilostane (0–1.0 μ M) in 0.02 M potassium phosphate buffer, pH 7.4. For 3 β -HSD2 and R195P-1, similar incubations contained DHEA (8.0 or 20.0 μ M) and trilostane (0–7.5 μ M). Dixon analysis (I vs. $1/V$) was used to determine the mode of inhibition and calculate the K_i values. (C) denotes a competitive mode of inhibition, and no notation indicates a noncompetitive mode of inhibition. Values from the triplicate experiments are shown using mean \pm SD.

protein. The R195P-1 mutation shifts the high-affinity, competitive inhibition profile of 3 β -HSD1 to a low-affinity ($K_i = 2.56 \mu$ M), non-competitive inhibition profile similar to that of 3 β -HSD2 containing Pro195. The P195R-2 mutation shifts the low-affinity, noncompetitive inhibition profile of 3 β -HSD2 to a high-affinity ($K_i = 0.19 \mu$ M), competitive inhibition profile similar to that of 3 β -HSD1 containing Arg195 (Table 2).

Comparisons of the Michaelis–Menten values of DHEA, 16 β -hydroxy-DHEA and 16 α -hydroxy-DHEA as substrates of 3 β -HSD1, 3 β -HSD2, R195P-1 and P195R-2 are shown in Table 3. The DHEA and 16 α -hydroxy-DHEA physiological substrates are utilized by 3 β -HSD1 with similar affinities. 3 β -HSD1 (containing Arg195) utilizes these substrates with 4.3-fold lower and 2.3-fold lower K_m values compared to those measured for 3 β -HSD2 (containing Pro195), respectively. The addition of the 16 β -hydroxyl group to DHEA decreases the substrate K_m by 2.6-fold for 3 β -HSD1 compared to DHEA. The P195R-2 mutant (3 β -HSD2 with Pro195 mutated to Arg195) has a 12.2-fold lower K_m value (higher affinity) for 16 β -hydroxy-DHEA compared to wild-type 3 β -HSD2. The R195P-1 mutant (3 β -HSD1 with Arg195 mutated to Pro195) has a 10.4-fold higher K_m value (lower affinity) for 16 β -hydroxy-DHEA compared to wild-type 3 β -HSD1. The P195R-2 and R195P-1 mutants shifted K_m values for DHEA and 16 α -hydroxy-DHEA similarly but to a lesser extent than measured for 16 β -hydroxy-DHEA (Table 3).

The K_m values measured for the coenzymes of the 3 β -HSD (NAD⁺) and isomerase (NADH) activities of the P195R-1 mutant are similar to those measured for wild-type 3 β -HSD1, and the coenzyme values measured for the P195R-2 mutant are similar to those measured for wild-type 3 β -HSD2 (Table 4). The structural model did not suggest an interaction of cofactor with Arg195 in 3 β -HSD1, which is consistent with these coenzyme kinetic measurements.

Table 3Comparison of Michaelis–Menten constants of 16 β -hydroxy-DHEA, 16 α -hydroxy-DHEA and DHEA as substrates for human R195P-1, 3 β -HSD1, P195R-2 and 3 β -HSD2.

Purified enzyme	DHEA ^a			16 β -hydroxy-DHEA			16 α -hydroxy-DHEA		
	K_m (μ M)	k_{cat} (min)	k_{cat}/K_m ($\text{min}^{-1} \mu\text{M}^{-1}$)	K_m (μ M)	k_{cat} (min)	k_{cat}/K_m ($\text{min}^{-1} \mu\text{M}^{-1}$)	K_m (μ M)	k_{cat} (min)	k_{cat}/K_m ($\text{min}^{-1} \mu\text{M}^{-1}$)
R195P-1	10.7	7.7	0.72	15.0	9.3	0.62	19.6	9.3	0.47
3 β -HSD1	3.7	3.3	0.89	1.4	2.9	2.07	6.4	5.8	0.90
P195R-2	7.7	5.6	0.73	1.5	3.2	2.13	4.0	4.6	1.15
3 β -HSD2	15.6	8.7	0.44	18.4	8.4	0.46	14.8	9.1	0.61

^a Kinetic constants for the 3 β -HSD substrates were determined spectrophotometrically (340 nm) in incubations containing DHEA, 16 β -hydroxy-DHEA or 16 α -hydroxy-DHEA (1–100 μ M), NAD⁺ (0.2 mM) and purified enzyme (0.04 mg) in 0.02 M potassium phosphate, pH 7.4. Mean kinetic values are shown from duplicate experiments with a range of $\leq 10\%$.

Table 4Cofactor kinetics for the 3 β -HSD and isomerase activities of the purified R195P-1, 3 β -HSD1, P195R-2 and 3 β -HSD2 enzymes.

Purified enzyme	3 β -HSD NAD ⁺ ^a			Isomerase NADH ^b		
	K_m (μ M)	k_{cat} (min)	k_{cat}/K_m ($\text{min}^{-1} \mu\text{M}^{-1}$)	K_m (μ M)	k_{cat} (min)	k_{cat}/K_m ($\text{min}^{-1} \mu\text{M}^{-1}$)
R195P-1	20.5	6.0	0.29	3.6	61.8	17.2
3 β -HSD1	34.1	3.5	0.10	4.6	45.0	9.8
P195R-2	56.4	10.5	0.19	5.5	89.5	16.3
3 β -HSD2	86.3	7.1	0.08	12.6	99.1	7.9

^a Kinetic constants for the 3 β -HSD cofactor were determined in incubations containing NAD⁺ (13–100 μ M), dehydroepiandrosterone (100 μ M) and purified enzyme (0.03 mg) in 0.02 M potassium phosphate, pH 7.4.

^b Kinetic constants for the isomerase cofactor were determined in incubations of NADH (3–50 μ M), 5-androstene-3,17-dione (100 μ M) and purified enzyme (0.02 mg) in 0.02 M potassium phosphate buffer, pH 7.4. Mean kinetic values are shown from duplicate experiments with a range of $\leq 12\%$.

Table 5Substrate kinetics for the 3 β -HSD and isomerase activities of the purified D61N, D61V, E192A, T8A and wild-type enzymes.

Purified enzyme	3 β -HSD ^a			Isomerase ^b		
	K_m (μ M)	k_{cat} (min)	k_{cat}/K_m ($\text{min}^{-1} \mu\text{M}^{-1}$)	K_m (μ M)	k_{cat} (min)	k_{cat}/K_m ($\text{min}^{-1} \mu\text{M}^{-1}$)
D61N	4.7	2.8	0.60	28.8	50.0	1.74
D61V	No activity			No activity		
E192A	30.4	1.8	0.06	19.8	16.9	0.85
T8A	8.2	3.6	0.44	27.9	44.4	1.59
3 β -HSD1	3.7	3.3	0.89	27.9	50.2	1.80

^a Kinetic constants for the 3 β -HSD substrate (DHEA) were determined in incubations containing NAD⁺ (100 μ M), dehydroepiandrosterone (2–100 μ M) and purified enzyme (0.03 mg) in 0.02 M potassium phosphate, pH 7.4.

^b Kinetic constants for the isomerase substrate (5-androstene-3,17-dione) were determined in incubations of NADH (50 μ M), 5-androstene-3,17-dione (16.67–100 μ M) and purified enzyme (0.02 mg) in 0.02 M potassium phosphate buffer, pH 7.4. Mean kinetic values are shown from duplicate experiments with a range of $\leq 10\%$.

3.4. Kinetic analyses of substrate and cofactor utilization by the wild-type and D61V, D61N, T8A and E192A mutant enzymes

Mutations of Asp61 in 3 β -HSD1 produced changes in the cofactor kinetics. The non-conservative mutation, D61V, completely abolished 3 β -HSD and isomerase activities of the enzyme, possibly due to misfolding of the protein. The more conservative mutation, D61N, produced a 1.3-fold increase in K_m for the DHEA substrate (Table 5), a 1.9-fold increase in K_m for NAD⁺ utilization by the 3 β -HSD activity (Table 6) and little change in isomerase kinetics for either substrate or cofactor.

The role of Asp192 as a potentially key residue for the binding of DHEA substrate by 3 β -HSD1 and 3 β -HSD2 has been clarified

by kinetic analyses in Tables 5 and 6. The E192A mutation caused a 8.2-fold increase in DHEA K_m and no change in the K_m for NAD⁺. The unchanged kinetic values measured for substrate and cofactor utilization for the T8A mutant compared to wild-type 3 β -HSD1 indicates that Thr8 does not play a role in this enzyme (Tables 5 and 6).

4. Discussion

Human 3 β -HSD1 has been overlooked as a target enzyme for inhibition in the treatment of breast cancer [22], possibly due to the presence of two isoforms in the human female. 3 β -HSD1

Table 6Cofactor kinetics for the 3 β -HSD and isomerase activities of the purified D61N, D61V, E192A, T8A and wild-type enzymes.

Purified enzyme	NAD 3 β -HSD ^a			NADH isomerase ^b		
	K_m (μ M)	k_{cat} (min)	k_{cat}/K_m ($\text{min}^{-1} \mu\text{M}^{-1}$)	K_m (μ M)	k_{cat} (min)	k_{cat}/K_m ($\text{min}^{-1} \mu\text{M}^{-1}$)
D61N	64.3	3.7	0.06	7.2	46.1	6.4
D61V	No activity			No activity		
E192A	35.1	1.6	0.05	2.5	18.8	7.5
T8A	33.3	2.7	0.08	6.5	41.8	6.4
3 β -HSD1	34.1	3.5	0.10	4.6	45.0	9.8

^a Kinetic constants for the 3 β -HSD cofactor were determined in incubations containing NAD⁺ (13–100 μ M), dehydroepiandrosterone (100 μ M) and purified enzyme (0.03 mg) in 0.02 M potassium phosphate, pH 7.4.

^b Kinetic constants for the isomerase cofactor were determined in incubations of NADH (2–50 μ M), 5-androstene-3,17-dione (50 μ M) and purified enzyme (0.02 mg) in 0.02 M potassium phosphate buffer, pH 7.4. Mean kinetic values are shown from duplicate experiments with a range of $\leq 12\%$.

is expressed in mammary gland, breast tumors, placenta and skin, while 3 β -HSD2 is expressed in the adrenal gland and ovary [23]. Because the inhibition of adrenal 3 β -HSD2 may decrease the production of cortisol and aldosterone in postmenopausal women, inhibition of 3 β -HSD1 in breast tumors to block estradiol production could produce undesirable side effects. However, we have shown that the classic 3 β -HSD inhibitors, trilostane and epostane, competitively inhibit purified human 3 β -HSD1 with 12–16-fold higher affinity compared to the noncompetitive inhibition of human 3 β -HSD2 by these compounds [12,24]. This study identifies an amino acid in the steroid binding domain of human 3 β -HSD1 that may be exploited to produce new inhibitors that are much more highly specific for 3 β -HSD1 in breast tumors compared to adrenal 3 β -HSD2, so the side effect of adrenal insufficiency may be avoided.

These kinetic analyses of the R195P-1 and P195R-2 mutant 3 β -HSD enzymes support a key role for Arg195 that produces high-affinity binding of human 3 β -HSD1 with the 17 β -hydroxyl group of the competitive inhibitor, trilostane, and the 17-keto group of the DHEA substrate. In contrast, the presence of Pro195 in 3 β -HSD2 apparently prevents this isoenzyme from binding these steroid ligands with high-affinity and produces a shift in the inhibition mode of trilostane to noncompetitive. It is especially noteworthy that the proposed dual interaction of the guanidinium R-group of Arg195 of the R195P-2 mutant of 3 β -HSD2 with the 16 β -hydroxy, 17-keto groups of 16 β -hydroxy-DHEA substrate produces substantially higher affinity binding (12.2-fold lower K_m values) for this substrate compared to wild-type 3 β -HSD2. Exploiting these interactions with Arg195 may produce highly selective inhibitors of 3 β -HSD1 that may be effective as new treatments for hormone-sensitive breast cancer.

The roles of other putative substrate and cofactor fingerprint residues have been clarified. The Asp192 residue of 3 β -HSD appears to interact with the 17-keto group of the DHEA substrate, and kinetic analyses of the E192A mutant support a role for this residue in substrate but not in cofactor utilization. In some members of the short-chain dehydrogenase reductase family, Thr12 functions with the NNAG (Asn-Asn-Ala-Gly) motif at residues 86–89 to bind solvent (water) and mutation of that Thr (T12A) disrupts enzyme function [10]. However, human 3 β -HSD lacks the NNAG motif [9]. Our kinetic analyses of the analogous Thr mutant, T8A, in human 3 β -HSD1 show that Thr8 is not a critical residue in this enzyme. The Arg61 residue in 3 β -HSD1 is analogous to Arg60 in bacterial 3 β ,17 β -hydroxysteroid dehydrogenase, which was shown by mutagenesis to hydrogen bond with the 6-amino group on the adenine of enzyme-bound NAD⁺ [10]. Our kinetic analyses with the D61N mutant of 3 β -HSD1 suggest that Asp61 may play a similar role in cofactor utilization in human 3 β -HSD1.

Understanding the structure/function relationships of the high-affinity inhibition of 3 β -HSD1 by trilostane may lead to the development of new, more specific inhibitors of 3 β -HSD1 that may be used to block the production of estradiol from DHEA in breast tumors without compromising steroidogenesis mediated by 3 β -HSD2 in the human adrenal enzyme. Based on the success of the aromatase inhibitors in treating hormone-sensitive breast tumors [25,26], the characterization of a new target enzyme in this biosynthetic pathway enhances our ability to develop new treatments for breast cancer.

Acknowledgments

This research was supported by NIH grant CA114717 (JLT). We thank Gavin P. Vinson, DSc, PhD, School of Biological Sciences, Queen Mary University of London, for the providing the trilostane.

References

- [1] E. Rheaume, Y. Lachance, H.-F. Zhao, N. Breton, M. Dumont, Y. de Launoit, C. Trudel, V. Luu-The, J. Simard, F. Labrie, Structure and expression of a new complementary DNA encoding the almost exclusive 3 beta-hydroxysteroid dehydrogenase/delta 5-delta 4-isomerase in human adrenals and gonads, *Mol. Endocrinol.* 5 (8) (1991) 1147–1157.
- [2] B. Persson, Y. Kallberg, J.E. Bray, E. Bruford, S.L. Dellaporta, A.D. Favia, R.G. Duarte, H. Jörnvall, K.L. Kavanagh, N. Kedishvili, M. Kisiela, E. Maser, R. Mindnich, S. Orchard, T.M. Penning, J.M. Thornton, J. Adamski, U. Oppermann, The SDR (short-chain dehydrogenase/reductase and related enzymes) nomenclature initiative, *Chem. Biol. Interact.* 178 (1–3) (2009) 94–98.
- [3] J.L. Thomas, R.P. Myers, R.C. Strickler, Human placental 3 β -hydroxy-5-ene-steroid dehydrogenase and steroid 5–4-ene-isomerase: purification from mitochondria and kinetic profiles, biophysical characterization of the purified mitochondrial and microsomal enzymes, *J. Steroid Biochem.* 33 (2) (1989) 209–217.
- [4] S. Gingras, R. Moriggl, B. Groner, J. Simard, Induction of 3beta-hydroxysteroid dehydrogenase/delta5-delta4 isomerase type 1 gene transcription in human breast cancer cell lines and in normal mammary epithelial cells by interleukin-4 and interleukin-13, *Mol. Endocrinol.* 13 (1) (1999) 66–81.
- [5] W.E. Rainey, B.R. Carr, H. Sasano, T. Suzuki, J.I. Mason, Dissecting human adrenal androgen production, *Trends Endocrinol. Metab.* 13 (6) (2002) 234–239.
- [6] J.L. Thomas, J.I. Mason, S. Brandt, B.R. Spencer, W. Norris, Structure/function relationships responsible for the kinetic differences between human type 1 and type 2 3beta-hydroxysteroid dehydrogenase and for the catalysis of the type 1 activity, *J. Biol. Chem.* 277 (45) (2002) 42795–42801.
- [7] H. Jörnvall, B. Persson, M. Krook, S. Atrian, R. Gonzalez-Duarte, J. Jeffery, D. Ghosh, Short-chain dehydrogenases/reductases (SDR), *Biochemistry* 34 (18) (1995) 6003–6013.
- [8] J.L. Thomas, W.L. Duax, A. Addlagatta, L. Scaccia, K.A. Fizzell, S.B. Carloni, Serine 124 completes the Tyr, Lys and Ser triad responsible for the catalysis of human type 1 3 β -hydroxysteroid dehydrogenase, *J. Mol. Endocrinol.* 33 (1) (2004) 253–261.
- [9] V.Z. Pletnev, J.L. Thomas, F.L. Rhaney, L.S. Holt, L.A. Scaccia, T.C. Umland, W.L. Duax, Rational proteomics V: structure-based mutagenesis has revealed key residues responsible for substrate recognition and catalysis by the dehydrogenase and isomerase activities in human 3 β -hydroxysteroid dehydrogenase/isomerase type 1, *J. Steroid Biochem. Mol. Biol.* 101 (1) (2006) 50–60.
- [10] C. Filling, K.D. Berndt, J. Benach, T. Knapp, T. Prozorovski, E. Nordling, R. Ladenstein, H. Jörnvall, U. Oppermann, Critical residues for structure and catalysis in short chain dehydrogenases/reductases, *J. Biol. Chem.* 277 (28) (2002) 25677–25684.
- [11] J.L. Thomas, R. Huether, V.L. Mack, L.A. Scaccia, R.C. Stoner, W.L. Duax, Structure/function of human type 1 3 β -hydroxysteroid dehydrogenase: an intrasubunit disulfide bond in the Rossmann-fold domain and a Cys residue in the active site are critical for substrate and coenzyme utilization, *J. Steroid Biochem. Mol. Biol.* 107 (1–2) (2007) 80–87.
- [12] J.L. Thomas, V.L. Mack, J.A. Glow, D. Moshkelani, K.M. Bucholtz, Structure/function of the inhibition of human 3 β -hydroxysteroid dehydrogenase type 1 and type 2 by trilostane, *J. Steroid Biochem. Mol. Biol.* 111 (1–2) (2008) 66–73.
- [13] J.B. Thoden, P.A. Frey, H.M. Holden, Crystal structures of the oxidized and reduced forms of UDP-galactose 4-epimerase isolated from *Escherichia coli*, *Biochemistry* 35 (16) (1996) 2557–2566.
- [14] R. Shi, S.X. Lin, Cofactor hydrogen bonding onto the protein main chain is conserved in the short chain dehydrogenase/reductase family and contributes to nicotinamide orientation, *J. Biol. Chem.* 279 (16) (2004) 16778–16785.
- [15] J.D. Thompson, D.G. Higgins, T.J. Gibson, CLUSTAL W: improving the sensitivity of progressive multiple sequence alignment through sequence weighting, position specific gap penalties and weight matrix choice, *Nucl. Acids Res.* 22 (22) (1994) 4673–4680.
- [16] G.M. Morris, D.S. Goodsell, R.S. Halliday, R. Huey, W.E. Hart, R.K. Belew, A.J. Olson, Automated docking using a Lamarckian genetic algorithm and empirical binding free energy function, *J. Comput. Chem.* 19 (14) (1998) 1639–1662.
- [17] J.L. Thomas, B.W. Evans, G. Blanco, R.W. Mercer, J.I. Mason, S. Adler, W.E. Nash, K.E. Isenberg, R.C. Strickler, Site-directed mutagenesis identifies amino acid residues associated with the dehydrogenase and isomerase activities of human type I (placental) 3 β -hydroxysteroid dehydrogenase/isomerase, *J. Steroid Biochem. Mol. Biol.* 66 (5–6) (1998) 327–334.
- [18] M.M. Bradford, A rapid and sensitive method for the quantitation of microgram quantities of protein utilizing the principle of protein-dye binding, *Anal. Biochem.* 72 (May) (1976) 248–254.
- [19] J.L. Thomas, E.A. Berko, A. Faustino, R.P. Myers, R.C. Strickler, Human placental 3 β -hydroxy-5-ene-steroid dehydrogenase and steroid 5–4-ene-isomerase: purification from microsomes, substrate kinetics, and inhibition by product steroids, *J. Steroid Biochem.* 31 (5) (1988) 785–793.
- [20] I.H. Segel, *Enzyme Kinetics: Behavior and Analysis of Rapid Equilibrium and Steady-State Enzyme Systems*, John Wiley & Sons, New York, 1993, pp. 109–111.
- [21] J.L. Thomas, W.L. Duax, A. Addlagatta, S. Brandt, R.R. Fuller, W. Norris, Structure/function relationships responsible for coenzyme specificity and the isomerase activity of human type 1 3 β -hydroxysteroid dehydrogenase/isomerase, *J. Biol. Chem.* 278 (37) (2003) 35483–35490.
- [22] J.R. Pasqualini, The selective estrogen enzyme modulators in breast cancer: a review, *Biochim Biophys. Acta* 1654 (2) (2004) 123–143.

- [23] J. Simard, F. Durocher, F. Mebarke, C. Turgeon, R. Sanchez, Y. Labrie, J. Couet, C. Trudel, E. Rheaume, Y. Morel, V. Luu-The, F. Labrie, Molecular biology and genetics of the 3β -hydroxysteroid dehydrogenase/ $\Delta 5$ - $\Delta 4$ isomerase gene family, *J. Endocrinol.* 150 (Suppl.) (1996) S189–S207.
- [24] J.L. Thomas, K.M. Bucholtz, J. Sun, V.L. Mack, B. Kacsoh, Structural basis for the selective inhibition of human 3β -hydroxysteroid dehydrogenase 1 in human breast tumor MCF-7 cells, *Mol. Cell Endocrinol.* 302 (1–2) (2009) 174–182.
- [25] R.J. Santen, S.J. Santner, R.J. Pauley, L. Tait, J. Kaseta, L.M. Demers, C. Hamilton, W. Yue, J.P. Wang, Estrogen production via the aromatase enzyme in breast carcinoma – which cell type is responsible, *J. Steroid Biochem. Mol. Biol.* 61 (3–6) (1997) 267–271.
- [26] S. Luo, C. Martel, S. Gauthier, Y. Merand, A. Belanger, C. Labrie, F. Labrie, Long-term inhibitory effects of a novel anti-estrogen on the growth of ZR-75-1 and MCF-7 human breast cancer tumors in nude mice, *Int. J. Cancer* 73 (3) (1997) 735–739.